Depletion of Pre-16S rRNA in Starved *Escherichia coli* Cells

GERARD A. CANGELOSI* AND WILLIAM H. BRABANT

*Seattle Biomedical Research Institute and Department of Pathobiology,
University of Washington, Seattle, Washington*

Specific hybridization assays for intermediates in rRNA synthesis (pre-rRNA) may become useful for monitoring the growth activity of individual microbial species in complex natural systems. This possibility depends upon the assumption that rRNA processing in microbial cells continues after growth and pre-rRNA synthesis cease, resulting in drainage of the pre-rRNA pool. This is not the case in many eukaryotic cells, but less is known about the situation in bacteria. Therefore, we used DNA probes to measure steady-state cellular pre-16S rRNA pools during growth state transitions in *Escherichia coli*. Pre-16S rRNA became undetectable when cells entered the stationary phase on rich medium and was replenished upon restoration of favorable growth conditions. These fluctuations were of much greater magnitude than concurrent fluctuations in the mature 16S rRNA pool. The extent of pre-16S rRNA depletion depended upon the circumstances limiting growth. It was significantly more pronounced in carbon-energy-starved cells than in nitrogen-starved cells or in cells treated with energy uncouplers. In the presence of the transcriptional inhibitor rifampin, rates of pre-16S rRNA depletion in carbon-energy-starved cells and nitrogen-starved cells were similar, suggesting that the difference between these conditions resides primarily at the level of pre-rRNA synthesis. Chloramphenicol, which inhibits the final steps in rRNA maturation, halted pre-16S rRNA depletion under all conditions. The data show that *E. coli* cells continue to process pre-rRNA after growth and *rrn* operon transcription cease, leading to drainage of the pre-rRNA pool. This supports the feasibility of using pre-rRNA-targeted probes to monitor bacterial growth in natural systems, with the caveat that patterns of pre-rRNA depletion vary with the conditions limiting growth.

In studies on complex natural systems such as infected host organisms, soil and aquatic communities, biofilms, and symbiotic associations, bacterial proliferation can be difficult to assess against a backdrop of uncontrollable biological and non-biological activities. As we seek to expand our understanding of bacterial physiology outside of the laboratory, there is increasing interest in identifying specific molecular markers which provide "snapshots" of the growth activity of individual microbial species in natural environments.

RNA molecules which are abundant in dividing cells but less so in resting cells may be useful molecular indicators of growth. If such molecules have species-specific sequences, they might provide specific information on the growth activity of individual microbial species present in highly complex samples. For example, specific mRNA molecules were used to assess the viability of noncultivable *Mycobacterium leprae* cells in animal tissues (26). Since bacterial mRNA can be difficult to detect and of undefined phylogenetic specificity, assays targeting bacterial rRNA have also been developed. Examples of the latter include growth studies on individual bacterial species in biofilms and ocean water (2, 8, 15, 27) and clinical antibiotic susceptibility tests of slow-growing *Mycobacterium* species (34). However, the resolving power of the rRNA approach is limited by the stability of mature rRNA. Even starved cells maintain stable ribosome pools so that growth can resume if conditions improve.

In light of these problems, assays targeting bacterial rRNA precursors (pre-rRNA) may be useful alternatives (4, 5, 19). Pre-rRNA molecules are intermediates in rRNA synthesis generated by RNase III cleavage of primary *rrn* operon transcripts. Leader and tail sequences are removed from the pre-rRNA during rRNA maturation and ribosome assembly to yield mature rRNA (16, 17, 24, 29). Pre-rRNAs are more abundant and easier to detect than even the most strongly expressed mRNA molecules in growing cells, but they are less persistent than mature rRNA in nongrowing cells. We described a diagnostic application of this concept in rapid antibiotic susceptibility testing of the slow-growing pathogen *Mycobacterium tuberculosis* (5). We were able to readily detect pre-16S rRNA in lysates of dividing *M. tuberculosis* cells by using conventional DNA probe or molecular amplification assays. The pre-rRNA disappeared rapidly from susceptible cells exposed to certain antituberculosis drugs but remained abundant in resistant cells. Probes for *M. tuberculosis* pre-rRNA had excellent phylogenetic specificity, suggesting that it may be possible to use such assays on unpurified samples.

In developing these methods, we noticed that pre-rRNA was difficult to detect in bacteria that had entered the stationary phase during normal growth without antibiotics. This observation lent support to proposals for the use of pre-rRNA to study the natural growth cycles of individual bacterial species in complex samples (19). It seemed unsurprising that pre-rRNA was depleted in bacterial cells upon cessation of growth due to inhibition of pre-rRNA synthesis coupled with ongoing processing. However, we could not find published data supporting the assumption that processing of existing pre-rRNA molecules continues after synthesis of new pre-rRNA ceases. This is not the case in many eukaryotic cells, which retard maturation of cytoplasmic rRNA when growth and rRNA synthesis cease and maintain stable pre-rRNA pools with only limited turnover (9, 10, 22). Moreover, 5S rRNA maturation in *Escherichia coli* was reported to be inhibited upon nutritional shift-down, resulting in accumulation of 9S precursor (12). Other studies on bacterial rRNA biogenesis did not address the fate of pre-rRNA upon cessation of wild-type growth (3, 6, 13, 16, 21, 23,

* Corresponding author. Mailing address: Seattle Biomedical Research Institute, 4 Nickerson St., Seattle, WA 98109. Phone: (206) 284-8846. Fax: (206) 284-0313. E-mail: cangelos@u.washington.edu.

TABLE 1. Probes used in this study

Probe	Target nucleotide positions[a]	Target description	Sequence	Probe design reference or source
ECPR1	3062–3091	3′ pre-16S rRNA tail (*rrnB*)	5′-GTGTGAGCACTACAAAGTACGCTTCTTTAA-3′	4[b]
ECPR2	3062–3091	3′ pre-16S rRNA tail (*rrnA*, *-D*, *-G*, and *-H*)	5′-GTGTGAGCACTGCAAAGTACGCTTCTTTAA-3′	This work
ECPR5	1432–1460	5′ pre-16S rRNA leader (*rrnA*, *-B*, *-C*, *-G*, and *-H*)	5′-ACTTGGTATTCATTTTTCGTCTTGCGACG-3′	4[c]
ECR2	1696–1723	Mature 16S rRNA	5′-GTCCCCCTCTTTGGTCTTGCGACGTTAT-3′	4[d]
ECR3	1564–1590	Mature 16S rRNA	5′-GTTACCGTTCGACTTGCATGTGTTAGG-3′	This work
UP041	1855–1874	Mature 16S rRNA (all prokaryotes)	5′-CTGCTGCCTCCCGTAGGAGT-3′	36

[a] Position numbers correspond to those for the *E. coli rrnB* operon (GenBank accession no. J01695). The mature 16S rRNA lies between positions 1518 and 3059.
[b] Probe ECPR1 was formerly EC012.
[c] Probe ECPR5 was formerly EC014.
[d] Probe ECR2 was formerly EC020.

25, 29, 30, 32). Transcript-based analyses of *rrn* promoter activity, such as that of Aviv et al. (3), detected the short-lived ($t_{1/2} = 20$ s) primary *rrn* transcript but not the more stable RNase III cleavage products termed pre-rRNA.

We set out to test the assumption that cessation of normal growth of wild-type bacteria is accompanied by measurable depletion of pre-rRNA. Consistent with this applied goal, we measured cellular pre-16S rRNA in *E. coli* by using DNA probe hybridization assays specific for precursor leader and tail sequences. We use the term depletion to refer to disappearance from cells of nucleic acid recognized by the probes. Depletion could result from a variety of different perturbations in equilibrium between pre-rRNA synthesis, processing, and degradation. To begin the process of resolving these possibilities, we also measured the effects of energy uncouplers and antibiotics on pre-rRNA depletion in growing and starved cells.

MATERIALS AND METHODS

Bacterial culture conditions and lysate preparation. *E. coli* type strain ATCC 11775 was cultured aerobically in Luria-Bertani (LB) broth or M9 minimal medium (28) at 37°C on rotary shakers. Where indicated (below), cultures were supplemented with 25 μg of rifampin per ml, 25 μg of chloramphenicol per ml, 1.25 mM 2,4-dinitrophenol (DNP), 50 mM potassium arsenate (KH_2AsO_4), or 50 μM carbonyl cyanide *m*-chlorophenylhydrazone (CCCP). At sampling time points, culture density was measured on a Milton Roy Spectronic 20S spectrophotometer, and 0.4-ml samples were pipetted into sterile, 2-ml polypropylene cryogenic vials containing 0.6 ml of a lysis-hybridization solution (150 mM Tris [pH 7.5], 30 mM EDTA, 3% *N*-lauroylsarcosine, 0.3% sodium dodecyl sulfate [SDS], 8.3% formamide, and 5 M guanidine thiocyanate). The tubes were mixed and immediately placed in an 85°C temperature block for 5 min, rapidly terminating RNA metabolism and lysing the cells (4). Guanidine lysates were stored at −70°C until use in hybridization assays.

Oligonucleotide probes. Oligonucleotide probes were synthesized by Amitof Biotech, Inc. (Boston, Mass.) or at MicroProbe Corporation (now Epoch Pharmaceuticals, Bothell, Wash.) with standard phosphoramidite chemistry on either an ABI 380B or Milligen 7500 automated DNA synthesizer and purified as described previously (35, 36). 5′-Hexylamine-tailed oligonucleotides used in sandwich hybridization assays were biotinylated (detection probes) or activated and attached to nylon beads (capture probes) as described previously (36). For slot blot assays, deprotected probes were end labeled with ^{32}P with T4 polynucleotide kinase (U.S. Biochemical) (5, 35).

Slot blot hybridization assays. Nucleic acid was extracted from 0.1 ml of each 1-ml guanidine lysate by a phenol-chloroform method and applied to Nytran Plus membrane filters (Schleicher and Schuell, Keene, N.H.) by using a slot blot apparatus, as described previously (5). Nucleic acid from approximately 1×10^7 to 3×10^7 cells was present on each blot, as calculated from culture optical density at harvest and an assumed cell density of 1×10^9 cells per ml at an optical density at 600 nm (OD_{600}) of 1.0. Hybridizations were carried out at 42°C in a formamide-SDS-Denhardt solution prepared with diethyl pyrocarbonate-treated water (5, 35). Filters were washed at 52°C in a solution containing 9 mM Tris (pH 8.0), 90 mM NaCl, 0.6 mM EDTA, and 0.2% SDS and exposed to Dupont NEN reflection autoradiography film for a few hours to several days, depending on target concentration and probe radioactivity. For visual presentation, autoradiograms were scanned on a Microtek 600Z scanner using Aldus Photostyler version 1.1a software. For numerical presentation, autoradiograms were scanned in the transmission mode on an LKB 2202 Ultroscan Laser Densitometer using the

LKB 2220 Recording Integrator for numerical raw data. Background was set at 0.2 reference absolute unit, as determined by manually scanning a blank area of each autoradiogram. Test runs of these parameters ensured that the weakest visible signals were recorded as peaks.

DNA probe sandwich hybridization assays. In DNA probe sandwich assays, target RNA was hybridized to capture probes tethered to activated nylon beads, followed by hybridization of biotinylated detection probes to separate sites on the captured RNA. Sandwiches of capture probe plus target RNA plus detection probe were detected by binding a streptavidin-alkaline phosphatase conjugate to the detection probe and incubating the sandwich with a chemiluminescent substrate, as described previously (4, 35, 36). Assays for pre-rRNA were carried out on undiluted lysates in 24-well tissue culture plates, and assays for total small subunit rRNA (total precursor or mature 16S rRNA) were carried out on lysates which had been diluted 50-fold in hybridization solution (3 M guanidine thiocyanate, 2% sarcosyl, 5% formamide, 50 mM Tris [pH 7.6], and 15 mM EDTA). Two hundred fifty microliters of each sample was added to a well containing five capture beads, and hybridization was carried out for 60 min at room temperature on a rotary platform set at 150 rpm. The solution was removed by aspiration and replaced with 300 μl of hybridization solution containing 5 μg of biotinylated detection probe per ml. Hybridization continued for 10 min. The solution was then replaced with 500 μl of blocking buffer (50 mM HEPES [pH 7.5], 100 mM NaCl, and 3.5% [vol/vol] gelatin [Sigma Chemical Co.], pasteurized at 85°C for 30 min). After 5 min of incubation, the blocking buffer was replaced with 300 μl of 0.1% (vol/vol) alkaline phosphatase-streptavidin (Vector Laboratories, Inc., Burlingame, Calif.) in blocking buffer. After 10 min of incubation, the beads were washed by two sequential 2-min incubations with 500 μl of assay wash (9 mM Tris, 1 mM EDTA, 90 mM NaCl, 1% [wt/vol] SDS, and 1% *N*-lauroylsarcosine [pH 8.0]), and an additional 2-min incubation with 500 μl of chemiwash solution (50 mM Tris, 100 mM NaCl, and 0.5% Tween 20, pasteurized at 85°C for 30 min). After final aspiration, the beads were transferred to a 96-well, white, flat-bottomed MicroFLUOR plate (Dynatech Laboratories, Chantilly, Va.) with one bead per well. One hundred microliters of Lumiphos 530 (Lumigen, Inc., Detroit, Mich.) was added to each well. The covered plates were incubated for 10 min, then read in a Labsystems Luminoskan luminometer. Luminometer values for each sample are averages for the five separate capture beads.

RESULTS

Hybridization assay formats. We used both autoradiographic slot blot assays and chemiluminescence sandwich assays to measure cellular pre-16S rRNA and total small subunit (SSU) rRNA pools in *E. coli*. In slot blot assays, extracted nucleic acid was applied to membrane filters and hybridized to individual oligonucleotide probes targeted to the 5′ pre-16S rRNA leader (probe ECPR5), the 3′ pre-16S rRNA tail (probes ECPR1 and ECPR2), and mature rRNA (probes ECR2, ECR3, and UP041) (Table 1). The probes were designed from published *E. coli* pre-rRNA and mature rRNA sequences (references 7, 17, and 18; GenBank/EMBL accession no. J01694, J01695, M10739, K00764, J01695, V00350, and D15061). BLAST searches (1) of sequence databases revealed no matches other than to the targeted *E. coli* pre-rRNA and mature rRNA sequences. Since pre-rRNA molecules contain the entire mature rRNA sequence, probes ECR2, ECR3, and UP041 detected the total SSU rRNA pool, which includes both

pre-16S rRNA and mature 16S rRNA. Between 90 and 99% of this pool is typically in the mature form in growing bacteria (16, 17).

We relied on the slot blot format for most experiments because of its superior signal-to-noise ratio and low cost. This format can in theory detect pre-rRNA leaders and tails even if they are present only as excised fragments, as opposed to intact precursors. In a subset of experiments, we also used a DNA probe sandwich hybridization assay for intact pre-16S rRNA. The sandwich assay has a capture probe (ECR2) and a detection probe (ECPR5) which recognize sites on either side of the 5′ mature pre-rRNA terminus, so that positive results require capture and detection of intact precursor molecules (4). To detect total SSU rRNA, we used a second sandwich assay with probes ECR3 and UP041, both of which hybridize to sites within the mature rRNA (Table 1).

Pre-rRNA and total SSU rRNA pools during growth state transitions on complex medium. We started our analysis by monitoring cellular pre-rRNA abundance during outgrowth from stationary phase on complex medium. Triplicate stationary-phase cultures grown on LB broth were diluted 20-fold into fresh broth. Samples taken at time points before and after dilution were rapidly lysed, and pre-16S rRNA and total SSU rRNA were measured in the lysates by using sandwich hybridization assays. Pre-16S rRNA was undetectable in stationary-phase cells, but dilution into fresh medium stimulated a rapid 50-fold increase in pre-rRNA per cell equivalent (Fig. 1A). Since the level of pre-rRNA in stationary-phase cells was below the detection limit of the assay, the actual increase may have been greater. Total SSU rRNA was more abundant than pre-rRNA throughout the experiment; however, total SSU rRNA per cell equivalent increased by a factor of only about 5 over the same time course.

In a similar experiment, stationary-phase cells were diluted 10-fold rather than 20-fold and monitored as described above. Although this led to less vigorous outgrowth, a rapid rise in pre-rRNA abundance was once again observed, accompanied by a more modest rise in total SSU rRNA (Fig. 1B). These patterns were even more apparent in slot blot hybridization assays conducted on the same samples (Fig. 1C). The 5′ pre-16S rRNA leader and the 3′ pre-16S rRNA tail, detected by separate probes, did not differ from each other in these responses. When exponential-phase cells growing on LB broth were allowed to enter the stationary phase, the opposite changes occurred. Pre-rRNA decreased ≥25-fold, to a level below the sandwich assay's sensitivity limit, while total SSU rRNA underwent a more modest decline (Fig. 2).

Effects of glucose and nitrogen starvation on pre-rRNA abundance. We next determined how limitation of individual nutrients affected the pre-rRNA pool. Cells were cultured to mid-logarithmic phase (OD_{600} = 0.25 to 0.40) on minimal (M9) medium containing glucose as the sole carbon-energy source and ammonium chloride as the sole nitrogen source. Aliquots were centrifuged and resuspended in complete M9 medium or M9 medium lacking glucose or ammonium. Aliquots shifted to incomplete media exhibited no further optical density growth (Fig. 3A). Samples taken over the course of 8.3 h after such shifts were analyzed for pre-16S rRNA and total SSU rRNA content by using slot blot hybridization assays. The extent of pre-16S rRNA depletion in glucose-starved cells (−G+N) appeared to exceed that in nitrogen-starved cells (+G−N) (ECPR5 [Fig. 3B]). Total SSU rRNA pools did not vary over this time course in any of the media (UP041 [Fig. 3B]).

Intensity of autoradiographic signals can vary with probe specific activity, autoradiographic exposure time, and other
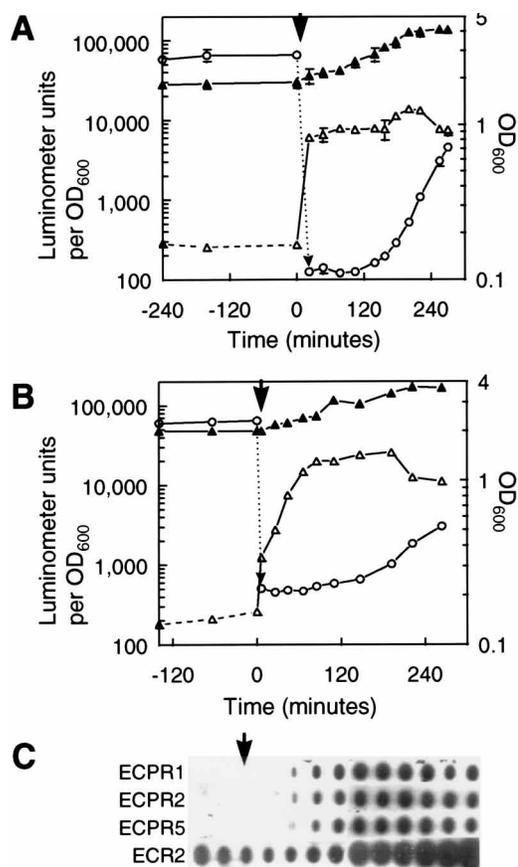

FIG. 1. Pre-16S rRNA and total SSU rRNA pools during outgrowth from stationary phase on LB broth. (A) Overnight cultures were diluted 20-fold into fresh broth at time zero (arrow). At time points before and after dilution, optical densities were recorded and samples were lysed for subsequent analysis by sandwich hybridization. Symbols: open circles, culture OD_{600} (right axis); open triangles, pre-16S rRNA per OD_{600} detected by an ECR2 plus ECPR5 sandwich (left axis); filled triangles, total SSU rRNA per OD_{600} detected by an ECR3 plus UP041 sandwich (left axis). Means and standard deviations of three parallel cultures are shown (some error bars did not exceed the diameters of the symbols). Datum points on the pre-16S rRNA curve connected by dashed lines were below background level. (B) A separate experiment in which a stationary-phase culture was diluted 10-fold rather than 20-fold. Symbols are the same as in panel A. (C) Slot blot hybridization assays for the 3′ pre-16S rRNA tail (ECPR1 and ECPR2), the 5′ pre-16S rRNA leader (ECPR5), and total SSU rRNA (ECR2) in nucleic acid extracted from the samples represented in panel B. Lysate concentrations were normalized to OD_{600} prior to extraction. Time points are the same as in panel B; dilution into fresh medium occurred at time zero (arrow). After hybridization, filter strips were exposed to a single autoradiographic film for 3 days. The autoradiogram was scanned, and images were aligned digitally to form the figure. Due to their stronger signal, the ECR2 blots were enhanced for more contrast than those of the other probes.

factors not related to biological activity, making it difficult to assess the reproducibility of slot blot results in visual terms. To express these results numerically and to facilitate comparison between experiments, we took advantage of the physiological uniformity of the cells at the outset of our experiments. All experiments except those represented in Fig. 1 and 2 began at time zero with exponential-phase cells grown on M9 medium (OD_{600} = 0.25 to 0.40 [Fig. 3A]). Autoradiograms were scanned in a densitometer, and outputs were expressed as percentages of the zero (exponential-phase) time points for each culture. Through this analysis, we found that the pre-16S rRNA pool declined by about 1 order of magnitude in cells deprived of nitrogen for 8.3 h, as well as in cells which had
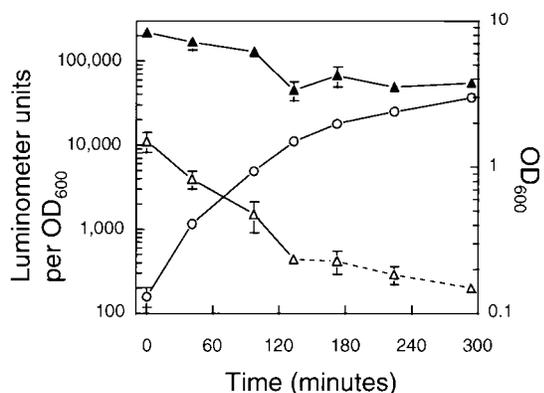
FIG. 2. Pre-16S rRNA and total SSU rRNA pools during the transition from exponential phase to stationary phase. Fluted 250-ml flasks containing 60 ml of LB broth were inoculated with 0.15 ml of an overnight culture and incubated on a rotary shaker at 37°C. At time zero (3 h after inoculation) and at the indicated time points thereafter, optical density was recorded and samples were lysed for subsequent pre-16S rRNA and total SSU rRNA analysis. Symbols: open circles, culture OD_{600} (right axis); open triangles, pre-16S rRNA per OD_{600} detected by an ECR2 plus ECPR5 sandwich (left axis); filled triangles, total SSU rRNA per OD_{600} detected by an ECR3 plus UP041 sandwich (left axis). Means and standard deviations of three parallel cultures are shown (some error bars did not exceed the diameters of the symbols). Datum points on the pre-16S rRNA curve connected by dashed lines were below background level.

entered the stationary phase on complete M9 medium over the same time period. In contrast, the pre-16S rRNA pool declined by 3 or more orders of magnitude in carbon-energy-starved cells (Fig. 3C). Total SSU rRNA abundance did not vary over this time period in any of the media (Fig. 3D).

Effects of energy uncouplers on pre-rRNA pools. A simple explanation for rapid pre-rRNA depletion in carbon-energy-starved cells might be that biosynthesis of the precursor requires more metabolic energy than does its processing. To test whether energy limitation brought about by other means also causes pre-rRNA depletion, we exposed exponential-phase cells growing aerobically on M9 medium to the energy uncouplers DNP, KH_2AsO_4, and CCCP. These agents were uniform in their effects, causing significant pre-16S rRNA depletion over the course of 3 h but to a lesser extent than glucose starvation (Fig. 4A). Thus, ATP limitation alone can only partially account for the strong depletion of pre-rRNA in glucose-starved cells. The limited extent of pre-rRNA depletion in uncoupler-treated cells does not reflect a significant ATP requirement for drainage of the pre-rRNA pool, since DNP and KH_2AsO_4 did not inhibit pre-rRNA depletion in glucose-starved cells (Fig. 4C). The total SSU rRNA pool did not vary under any of these conditions. (Fig. 4B and D).

Effects of antibiotics on pre-rRNA depletion in starved cells. Depletion of pre-rRNA in starved cells may occur through normal rRNA maturation mechanisms or, alternatively, through degradation or turnover. To help distinguish between these possibilities, we exposed cells to chloramphenicol, which inhibits the final steps in rRNA maturation (11, 24). When added to cultures 30 min after addition of uncoupling agents, chloramphenicol immediately halted pre-16S rRNA depletion, a result consistent with a predominant role for rRNA maturation in depletion of pre-rRNA under these conditions (Fig. 5B and C). When added to ammonium- and glucose-starved cultures, the drug not only halted depletion but also stimulated transient increases in pre-rRNA content (Fig. 5E and F), possibly
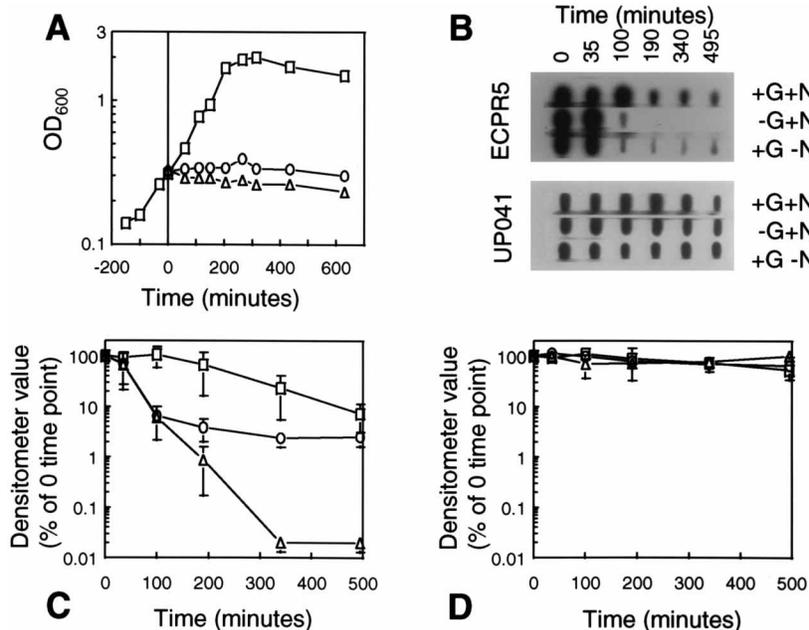

FIG. 3. Effects of glucose and nitrogen starvation on pre-16S rRNA and total SSU rRNA pools. Exponential-phase cells on complete M9 medium were shifted at time zero to medium lacking individual nutrients or to complete M9 medium, as described in the text. (A) Culture OD_{600}. Symbols: squares, complete M9 medium; circles, M9 medium lacking ammonium; triangles, M9 medium lacking glucose. (B) Slot blot hybridization assays for 5′ pre-16S rRNA (probe ECPR5; 48-h exposure) and total SSU rRNA (probe UP041; 4-h exposure) in cultures shifted to complete or incomplete media as shown in panel A. Samples were normalized to 3×10^7 cell equivalents prior to application on filters. Time points, in minutes, after shift-down are shown at the top. Abbreviations: +G+N, complete M9 medium; −G+N, M9 medium lacking glucose; +G−N, M9 medium lacking ammonium. Replicate filters probed with ECPR1 plus ECPR2 (3′ pre-16S rRNA) yielded results identical to those with ECPR5. (C) Numerical expression of slot blot results obtained with ECPR5. Densitometry values are expressed as percentages of zero (exponential-phase) time points as described in the text. Symbols: squares, +G+N; circles, +G−N; triangles, −G+N. Means and standard deviations of three experiments are shown, one of which was the experiment represented in panel B. (D) Numerical expression of slot blot results obtained with UP041 (total SSU rRNA). Symbols are the same as in panel C, and means and standard deviations of the same three cultures are shown.
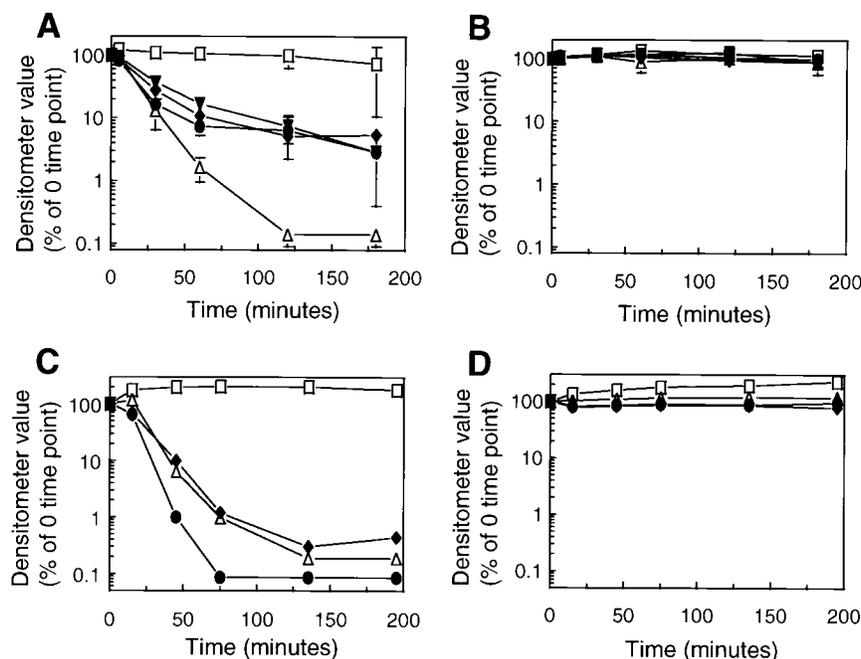
FIG. 4. Effects of energy uncouplers on pre-16S rRNA (detected by probe ECPR5) and total SSU RNA (detected by probe UP041) in growing and starved cells. Slot blot results are expressed as percentages of zero (exponential-phase) time points as described in the legend to Fig. 3. (A) At time zero, exponential-phase cultures were centrifuged and resuspended in complete M9 medium (+G+N) (open squares), +G+N medium supplemented with DNP (filled circles), +G+N medium supplemented with CCCP (filled inverted triangles), +G+N medium supplemented with KH$_2$AsO$_4$ (filled diamonds), or M9 medium lacking glucose (−G+N medium) (open triangles). Means and standard deviations of two experiments are shown. (B) Total SSU rRNA detected by probe UP041 in the same samples as those represented in panel A. (C) The effects of uncouplers on pre-16S rRNA depletion in glucose-starved cells. At time zero, exponential-phase cells were centrifuged and resuspended in +G+N medium (open squares), −G+N medium (open triangles), −G+N medium supplemented with DNP (filled circles), or −G+N medium supplemented with KH$_2$AsO$_4$ (filled diamonds). Identical results were obtained with probes ECPR1 and ECPR2. (D) Total SSU rRNA detected by probe UP041 in the same samples as those represented in panel C.

through inhibition of guanosine tetraphosphate synthetase I activity and relaxation of *rrn* operon transcription (33).

To determine whether rates of pre-rRNA processing vary with starvation conditions, we exposed growing, glucose-starved, and nitrogen-starved cultures to the transcriptional inhibitor rifampin and monitored depletion of pre-16S rRNA in the absence of further transcription (4, 5, 16). Under these conditions, depletion was no slower in nitrogen-starved cells than in glucose-starved cells (Fig. 6). Therefore, the difference between the effects of nitrogen and glucose starvation more likely resides at the level of input into the pre-rRNA pool than at the level of drainage of the pool.

DISCUSSION

The use of pre-rRNA-targeted probes to assess bacterial growth activity was proposed at least as early as 1984 (19), but it has not been put into widespread practice. The idea is based on the core assumption that rRNA maturation in bacterial cells continues after growth and pre-rRNA synthesis cease, resulting in depletion of the pre-rRNA pool. However, we could not find published data directly supporting this assumption for bacteria. The opposite situation exists in eukaryotic systems, which retard maturation of cytoplasmic pre-rRNA upon cessation of growth and maintain pools of stable pre-rRNA (9, 10, 22). The same has been reported of 5S rRNA maturation in *E. coli* (12). To help clarify the issue, we set out to characterize the physiological fate of pre-rRNA in starved *E. coli* cells.

Consistent with the practical motivation for this work, we used direct DNA hybridization to measure steady-state pre-rRNA pools in bacterial lysates. Cross-hybridizing activities were unlikely to account for our observations for several reasons. First, two probes were used in most experiments, one of which (ECPR5) targeted the 5′ pre-16S rRNA leader, while the other (ECPR1 and its near-homolog, ECPR2) targeted the 3′ pre-16S rRNA tail. There was complete agreement between the two. Second, two different hybridization formats were used in a subset of experiments, also with complete agreement. Third, our observations were consistent with previous descriptions of pre-rRNA in dividing cells as measured by other methods (16, 17, 21, 24, 25, 30). These descriptions of pre-rRNA include its lower abundance than mature rRNA, its rapid decline upon exposure to rifampin, and its rapid accumulation upon exposure to chloramphenicol. It is unlikely that artifactual activities would share all of these characteristics with pre-rRNA. Fourth, our methods did not differ significantly from standard methods for DNA probe detection of mature rRNA, which have been specific and reproducible in countless applications (2, 6, 8, 19, 31, 35, 37). Uncertainties related to rRNA secondary structure were also minimized by the use of multiple probes and hybridization formats.

The pre-16S rRNA pool was far more sensitive to growth physiology than was the total SSU rRNA pool, lending support to the core assumption behind the use of pre-rRNA probes to monitor bacterial growth. Even under conditions of relatively modest pre-rRNA depletion, for example, in nitrogen-starved cells, a ≥10-fold drop relative to actively growing cells was always observed (longer periods of nitrogen starvation led to larger drops). Therefore, pre-rRNA assays may provide useful information on the physiology of bacterial species in complex samples, especially if results can be expressed relative to more
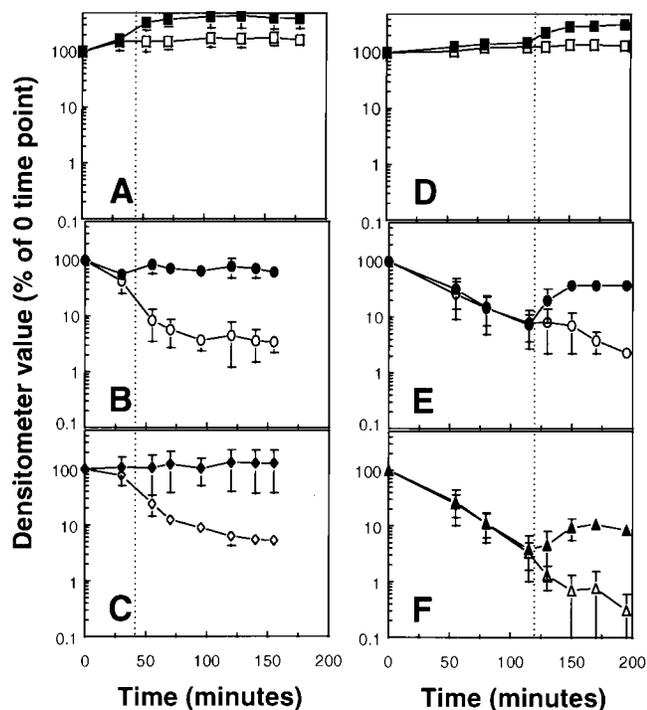
FIG. 5. Effects of chloramphenicol on pre-16S rRNA depletion as detected by probe ECPR5. (A, B, and C) Effects of chloramphenicol on pre-16S rRNA depletion in uncoupler-treated cells. At time zero, exponential-phase cultures on complete M9 medium (+G+N medium) were divided into three pairs of aliquots, centrifuged, and resuspended in +G+N medium (A), +G+N medium supplemented with DNP (B), or +G+N medium supplemented with KH_2AsO_4 (C). Thirty minutes after supplementation (vertical dotted line), chloramphenicol was added to one of each pair of cultures (filled symbols). (D, E, and F) Effects of chloramphenicol on pre-16S rRNA in starved cells. At time zero, exponential-phase cultures on +G+N medium were divided into three pairs of aliquots, centrifuged, and resuspended in +G+N medium (D), M9 medium lacking ammonium (+G−N medium) (E), or M9 medium lacking glucose (−G+N medium) (F). One hundred twenty minutes after these shifts (vertical dotted line), chloramphenicol was added to one of each pair of cultures (filled symbols). Slot blot results are expressed as percentages of zero (exponential-phase) time points as described in the legend to Fig. 3. Means and standard deviations of two experiments are shown in each graph. An additional run of each experiment yielded similar results but was not incorporated into these graphs because of slightly different timing of the chloramphenicol addition. Replicates of the experiments represented in panels D to F were also probed with ECPR1 and ECPR2, with identical results. Replicates of all filters probed with UP041 (total SSU rRNA) yielded flat curves, as in Fig. 3D, 4B, and 4D.

stable markers such as total SSU rRNA or genomic DNA. However, in considering such applications, it is important to bear in mind that fluctuations in the pre-rRNA pool vary quantitatively with the conditions limiting growth. This is consistent with the physiological diversity of starvation in bacteria (20).

Our results confirm a difference in pre-rRNA pools between glucose- and nitrogen-starved cells but do not fully explain it. The pre-rRNA pool is maintained by the equilibrium between input into the pool (transcription initiation and elongation) and drainage of the pool (rRNA maturation and nucleolytic turnover). It is most straightforward to hypothesize a greater role for the rate of input, in part because no mechanisms for regulating drainage have been described for bacteria. Moreover, drainage of the pre-rRNA pool in the presence of rifampin was no slower in nitrogen-starved cells than in glucose-starved cells, suggesting that these conditions differ primarily in their effects on input. A possible explanation for the partic-

ularly dramatic effects of carbon-energy starvation is that input requires more metabolic energy than does drainage. Consistent with this notion, energy uncouplers partially mimicked the effects of glucose starvation; however, additional factors are likely to be at least as important. A strong candidate is stringent control of stable RNA synthesis, which is known to be particularly pronounced in carbon-energy-starved cells (6, 14). The picture will be clarified further by independent measurement of input and drainage activities in wild-type cells and in mutants affected in the pathways that control rRNA biogenesis.

Uncoupling agents did not inhibit pre-rRNA depletion in glucose-starved cells, suggesting that depletion proceeds in such cells without a significant requirement for ATP synthesis. This is consistent with a previous report of functional pre-23S rRNA processing in cell-free systems lacking added ATP (29), and it fits with the notion of continuous, unregulated drainage of the pre-rRNA pool in vivo. However, we cannot yet completely rule out the possibility that rRNA processing can be arrested in response to specific natural growth conditions. In fact, maturation of the 5S rRNA subunit was reported to be repressed in *E. coli* cells shifted to salt buffer, leading to accumulation of 9S precursor in nongrowing cells (12). The apparent disparity between this observation and ours may reflect differences in rRNA subunit processing pathways, in timing of measurements, or in culture downshift conditions.

Chloramphenicol, which inhibits pre-rRNA processing and ribosome assembly (11, 24), halted pre-rRNA depletion in uncoupler-treated cells. This observation supports the hypothesis that normal rRNA maturation (as opposed to unknown pre-rRNA turnover pathways) is the major avenue of pre-rRNA drainage in such cells. The effects of chloramphenicol on the pre-rRNA pool in glucose- and nitrogen-starved cells were also consistent with this notion; however, in these cases the picture was complicated by transient accumulation of pre-rRNA in chloramphenicol-treated cells, possibly through inhibition of guanosine tetraphosphate synthesis and relaxation of stringent control (33).

In analyses of *Mycobacterium smegmatis* and *M. tuberculosis*, we observed patterns similar to those reported here during growth state transitions on complex media and exposure to
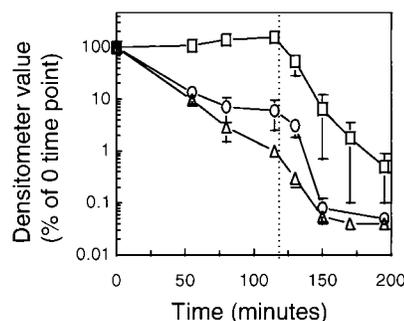

FIG. 6. Effects of rifampin on pre-16S rRNA (detected by probe ECPR5) in growing and starved cells. At time zero, exponential-phase cultures on complete M9 medium (+G+N medium) were centrifuged and resuspended in +G+N medium (squares), M9 medium lacking ammonium (+G−N medium) (circles), or M9 medium lacking glucose (−G+N medium) (triangles). One hundred twenty minutes after these shifts, rifampin was added to all cultures (vertical dotted line). Slot blot results are expressed as percentages of zero (exponential-phase) time points as described in the legend to Fig. 3. Means and standard deviations of two experiments are shown. An additional experiment yielded similar results but was not incorporated into the graph because of slightly different timing of the rifampin addition. Replicates of filters probed with ECPR1 and ECPR2 yielded identical results. Replicates of filters probed with UP041 (total SSU rRNA) yielded flat curves, as in Fig. 3D, 4B, and 4D.

energy uncouplers (unpublished data). While this is a limited number of species, the phylogenetic and physiological gaps between *Escherichia* and *Mycobacterium* are wide (38), and the patterns of pre-rRNA maintenance reported here do not appear to be confined to *E. coli* and similar rapidly growing species. In contrast to known eukaryotic examples (2, 10, 22), pre-rRNA pools in these bacteria are dramatically depleted under some (and perhaps most) conditions of growth limitation. This supports the core assumption behind proposals for the use of pre-rRNA probes to monitor bacterial growth in natural systems, with the important caveat that pre-rRNA fluctuations vary quantitatively with the conditions limiting growth. Characterization of pre-rRNA pools under additional conditions, and in additional microbial species, will further define the types of information obtainable by using such probes.

REFERENCES

1. **Altschul, S. F., W. Gish, W. Miller, E. W. Myers, and D. J. Lipman.** 1990. Basic local alignment search tool. J. Mol. Biol. **215:**403–410.
2. **Amann, R. I., W. Ludwig, and K. Schleifer.** 1995. Phylogenetic identification and in situ detection of individual microbial cells without cultivation. Microbiol. Rev. **59:**143–169.
3. **Aviv, M., H. Giladi, A. B. Oppenheim, and G. Glaser.** 1996. Analysis of the shut-off of ribosomal RNA promoters in *Escherichia coli* upon entering the stationary phase of growth. FEMS Microbiol. Lett. **140:**71–76.
4. **Britschgi, T. B., and G. A. Cangelosi.** 1994. Detection of rifampin-resistant bacteria using DNA probes for precursor rRNA. Mol. Cell. Probes **9:**19–24.
5. **Cangelosi, G. A., W. H. Brabant, T. B. Britschgi, and C. W. Wallis.** 1996. Detection of rifampin- and ciprofloxacin-resistant *Mycobacterium tuberculosis* by using species-specific assays for precursor rRNA. Antimicrob. Agents Chemother. **40:**1790–1795.
6. **Condon, C., C. Squires, and C. L. Squires.** 1995. Control of rRNA transcription in *Escherichia coli*. Microbiol. Rev. **59:**623–645.
7. **Dams, E., L. Hendricks, V. Van de Peer, J. M. Neefs, G. Smits, I. Vandenkempt, and R. De Wachter.** 1988. Compilation of small ribosomal subunit RNA sequences. Nucleic Acids Res. **16**(Suppl.):r87–r174.
8. **DeLong, E. F., G. S. Wickham, and N. R. Pace.** 1989. Phylogenetic stains: ribosomal RNA-based probes for the identification of single cells. Science **243:**1360–1363.
9. **Dudov, K. P., and M. D. Dabeva.** 1983. Post-transcriptional regulation of ribosome formation in the nucleus of regenerating rat liver. Biochem. J. **210:**183–192.
10. **Eckert, W. A., and W. Kaffenberger.** 1980. Regulation of rRNA metabolism in *Tetrahymena pyrifromis*. I. Nutritional shift-down. Eur. J. Cell Biol. **21:**53–62.
11. **Forget, B. G., and B. Jordan.** 1969. 5S RNA synthesized by *Escherichia coli* in presence of chloramphenicol: different 5′-terminal sequences. Science **167:**382–384.
12. **Georgellis, D., S. Arvidson, and A. von Gabain.** 1992. Decay of *ompA* mRNA and processing of 9S RNA are immediately affected by shifts in growth rate, but in opposite manners. J. Bacteriol. **174:**5382–5390.
13. **Ghora, B. K., and D. Apirion.** 1979. Identification of a novel RNA molecule in a new RNA processing mutant of *Escherichia coli* which contains 5S rRNA sequences. J. Biol. Chem. **254:**1951–1956.
14. **Jensen, K. F., and S. Pedersen.** 1990. Metabolic growth rate control of *Escherichia coli* may be a consequence of subsaturation of the macromolecular biosynthetic apparatus with substrates and catalytic components. Microbiol. Rev. **54:**89–100.
15. **Kerkhof, L., and B. B. Ward.** 1993. Comparison of nucleic acid hybridization and fluorometry for measurement of the relationship between RNA/DNA ratio and growth rate in a marine bacterium. Appl. Environ. Microbiol. **59:**1303–1309.
16. **King, T. C., and D. Schlessinger.** 1983. S1 nuclease mapping analysis of ribosomal RNA processing in wild type and processing deficient *Escherichia coli*. J. Biol. Chem. **258:**12034–12042.
17. **King, T. C., R. Sirdeskmukh, and D. Schlessinger.** 1986. Nucleolytic processing of ribonucleic acid transcripts in prokaryotes. Microbiol. Rev. **50:**428–451.
18. **Klein, B. K., A. Staden, and D. Schlessinger.** 1985. Electron microscopy of secondary structure in partially denatured precursor and mature *Escherichia coli* 16S and 23S rRNA. J. Biol. Chem. **260:**8114–8120.
19. **Kohne, D. E.** 1984. Method for detecting, identifying, and quantitating organisms and viruses. European patent 0 531 798.
20. **Kolter, R., D. A. Siegele, and A. Tormo.** 1993. The stationary phase of the bacterial life cycle. Annu. Rev. Microbiol. **47:**855–874.
21. **Krych, M., R. Sirdeshmukh, R. Gourse, and D. Schlessinger.** 1987. Processing of *Escherichia coli* 16S rRNA with bacteriophage lambda leader sequences. J. Bacteriol. **169:**5523–5529.
22. **Larson, D. E., P. Zahradka, and B. H. Sells.** 1991. Control points in eukaryotic ribosome biogenesis. Biochem. Cell Biol. **69:**5–22.
23. **Mackow, E. R., and F. N. Chang.** 1985. Processing of precursor ribosomal RNA and the presence of a modified ribosome assembly scheme in *Escherichia coli* relaxed strain. FEBS Lett. **182:**407–412.
24. **Pace, N. R.** 1973. Structure and synthesis of the ribosomal ribonucleic acid of prokaryotes. Bacteriol. Rev. **37:**562–603.
25. **Pace, N. R., and A. B. Burgin.** 1990. Processing and evolution of the rRNAs, p. 417–425. *In* W. E. Hill, A. Dahlberg, R. A. Garrett, P. B. Moore, D. Schlessinger, and J. R. Warner (ed.), The ribosome: structure, function, and evolution. American Society for Microbiology, Washington, D.C.
26. **Patel, B. K. R., D. K. Banerjee, and P. D. Butcher.** 1993. Determination of *Mycobacterium leprae* viability by polymerase chain reaction amplification of 71-kDa heat shock protein mRNA. J. Infect. Dis. **168:**799–800.
27. **Poulsen, L. K., G. Ballard, and D. A. Stahl.** 1993. Use of rRNA fluorescence in situ hybridization for measuring the activity of single cells in young and established biofilms. Appl. Environ. Microbiol. **59:**1354–1360.
28. **Sambrook, J., E. F. Fritsch, and T. Maniatis.** 1989. Molecular cloning: a laboratory manual, 2nd ed. Cold Spring Harbor Laboratory Press, Cold Spring Harbor, N.Y.
29. **Srivastava, A. K., and D. Schlessinger.** 1988. Coregulation of processing and translation: mature 5′ termini of *Escherichia coli* 23S ribosomal RNA form in polysomes. Proc. Natl. Acad. Sci. USA **85:**7144–7148.
30. **Srivastava, A. K., and D. Schlessinger.** 1990. rRNA processing in *Escherichia coli*, p. 426–434. *In* W. E. Hill, A. Dahlberg, R. A. Garrett, P. B. Moore, D. Schlessinger, and J. R. Warner (ed.), The ribosome: structure, function, and evolution. American Society for Microbiology, Washington, D.C.
31. **Stahl, D. A., B. Flesher, H. R. Mansfield, and L. Montgomery.** 1988. Use of phylogenetically based hybridization probes for studies of ruminal microbial ecology. Appl. Environ. Microbiol. **54:**1079–1084.
32. **Steen, R., D. K. Jemiolo, R. H. Skinner, J. J. Dunn, and A. E. Dahlberg.** 1986. Expression of plasmid-coded mutant ribosomal RNA in *E. coli*: choice of plasmid vectors and gene expression systems. Prog. Nucleic Acid Res. Mol. Biol. **33:**1–18.
33. **Svitil, A. L., M. Cashel, and J. W. Zyskind.** 1993. Guanosine tetraphosphate inhibits protein synthesis in vivo. A possible protective mechanism for starvation stress in *Escherichia coli*. J. Biol. Chem. **268:**2307–2311.
34. **van der Vliet, G. M. E., P. Schepers, R. A. F. Scukkink, B. van Gemen, and P. R. Klatser.** 1994. Assessment of mycobacterial viability by RNA amplification. Antimicrob. Agents Chemother. **38:**1959–1965.
35. **Van Ness, J., and L. Chen.** 1991. The use of oligodeoxynucleotide probes in chaotrope-based hybridization solutions. Nucleic Acids Res. **19:**5143–5151.
36. **Van Ness, J., S. Kalbfleisch, C. R. Petrie, M. W. Reed, J. C. Tabone, and N. M. J. Vermeulen.** 1991. A versatile solid support system for oligonucleotide probe-based hybridization. Nucleic Acids Res. **19:**3345–3350.
37. **Wagner, M., R. Erhart, W. Manz, R. Amann, H. Lemmer, D. Wedi, and K. Schleifer.** 1994. Development of an rRNA-targeted oligonucleotide probe specific for the genus *Acinetobacter* and its application for in situ monitoring in activated sludge. Appl. Environ. Microbiol. **60:**792–800.
38. **Wheeler, P. R., and C. Ratledge.** 1994. Metabolism of *Mycobacterium tuberculosis*, p. 353–385. *In* B. R. Bloom (ed.), Tuberculosis: pathogenesis, protection, and control. ASM Press, Washington, D.C.